

# Channel coupling effects in $\rho$ -meson photoproduction.

A. Usov\* and O. Scholten†

*Kernfysisch Versneller Instituut, University of Groningen, 9747 AA, Groningen, The Netherlands*

We investigate  $\rho$ -meson photoproduction in a coupled-channels formulation. It is shown that channel coupling effects are large and account for discrepancies observed in several single-channel treatments.

## I. INTRODUCTION

A number of experiments on vector meson production at low energies [1, 2, 3, 4] performed in recent years have greatly stimulated theoretical research on the subject [5, 6, 7, 8, 9, 10, 11, 12, 13, 14]. The investigation of vector meson production is expected to provide insight in the problem of “missing resonances” [15], as many of the predicted resonant states are believed to couple weakly to the pion channel, but should be visible in other reaction channels. Furthermore, in our previous analysis of photo-induced kaon production [16] we saw that the inclusion of the pion-induced  $\rho$ -meson production channel has a strong influence on pion scattering and  $K - \Lambda$  photoproduction cross-sections, but the detailed analysis of  $\rho$ -meson production was not done at that time. Therefore, in the current paper, we concentrate primarily on the analysis of  $\rho$ -meson production and its effects in a coupled channels calculation.

Most of the work done on vector meson production concentrated primarily on  $\omega$ -meson production. While most of the analyses performed so far employed tree-level models [8, 9, 10, 11, 12, 14], there are strong indications for the importance of channel coupling effects (loop corrections) for  $\omega$ -meson production [13]. A number of calculations performed using the K-matrix approach [5, 6, 7] included the  $\omega$ -production channels, but the magnitude of the contributions due to channel coupling was not investigated explicitly. The analyses of  $\omega$ - and  $\rho$ -meson production channels in the “effective quark model Lagrangian” approach [8] have found a good simultaneous description of the data at the time, however these do not include the coupling to the pion sector, which was found to be essential [13]. In general, tree-level models have difficulties [14] describing the differential cross-section in the region of high momentum transfer. We show that coupled-channels treatment of the photo-induced  $\rho$ -meson production is able to account for a major part of the discrepancies observed in a single-channel model. The coupling to the pion-nucleon state is by far the most important ingredient.

In Section II we give a brief outline of our model and in Section III we present and discuss the results of the calculation.

## II. MODEL

The model used in this work is based on an effective Lagrangian formalism. The detailed description of the model can be found in our previous paper [16], here we will summarize it, give a description of the  $\gamma + N \rightarrow \rho + N$  and  $\pi + N \rightarrow \rho + N$  reaction channels and specify the modifications made to other reaction channels in order to extend the applicability of the model to higher energies.

Our model is based on the K-matrix formalism to implement channel coupling. A discussion of the K-matrix formalism can be found in ref. [16] and references therein. The use of the K-matrix formalism allows to generate an infinite, non-perturbative set of loop corrections for states explicitly included in the model, while obeying a number of symmetries like gauge invariance, unitarity and crossing symmetry. The model space used in the present investigation is formed by  $K - \Lambda$ ,  $K - \Sigma$ ,  $\phi - N$ ,  $\eta - N$ ,  $\gamma - N$ ,  $\pi - N$  and  $\rho - N$  states. A number of non-strange resonances are included in s- and u-channel contributions. For the complete list of the included resonances and their parameters we refer to our previous publication [16].

Parameters entering the calculation are mostly unchanged as compared to what was presented in our previous calculation [16]. The most important exceptions are the  $NN\omega$  coupling constant and a few cut-offs in the pion photoproduction channel. In Table I we quote the values of the parameters relevant for the current discussion.

In the following sections we use a notation where  $p$ ,  $k$ ,  $p'$  and  $-q$  correspond to the initial proton,  $\rho$ -meson and final proton and photon(pion) 4-momenta respectively. Indices  $\mu$  and  $\nu$  label the photon- and  $\rho$ -meson polarization indices. We assume that the meson momenta are directed into the vertex, so that energy-momenta conservation reads as  $p + k = p' - q$ .

The complete Lagrangian is given in ref. [16] and here we quote only the terms relevant for the current discus-

---

\*Electronic address: usov@kvi.nl

†Electronic address: scholten@kvi.nl

TABLE I: Parameters summary table

$g_{NN\pi}$	13.47	$g_{\rho\pi\pi}$	6
$g_{NN\eta}$	3	$g_{\rho\pi^0\gamma}$	-0.12
$g_{NN\sigma}$	10	$g_{\rho\pi^\pm\gamma}$	-0.10
$g_{NN\rho}$	2.2	$g_{\rho\eta\gamma}$	0.22
$g_{NN\omega}$	3.0	$g_{\omega\pi\gamma}$	0.32
		$g_{\rho\sigma\gamma}$	12

sion.

$$\begin{aligned}
\mathcal{L}_{NN\pi} &= ig_{NN\pi}\bar{N}\frac{(\chi\vec{\pi} + i\vec{\partial}\vec{\pi}/2M)\cdot\vec{\tau}}{\chi+1}\gamma^5 N \\
\mathcal{L}_{NN\eta} &= ig_{NN\eta}\bar{N}\frac{\chi\eta + i\vec{\partial}\eta/2M}{\chi+1}\gamma^5 N \\
\mathcal{L}_{NN\sigma} &= -g_{NN\sigma}\bar{N}\sigma N \\
\mathcal{L}_{NN\rho} &= -g_{NN\rho}\bar{N}\left(\gamma_\mu\vec{\rho}^\mu + \frac{\kappa_\rho}{2M}\sigma_{\mu\nu}\partial^\nu\vec{\rho}^\mu\right)\cdot\vec{\tau}N \\
\mathcal{L}_{NN\omega} &= -g_{NN\omega}\bar{N}\left(\gamma_\mu\omega^\mu + \frac{\kappa_\omega}{2M}\sigma_{\mu\nu}\partial^\nu\omega^\mu\right)N \\
\mathcal{L}_{NN\gamma} &= -e\bar{N}\left(\frac{1+\tau_0}{2}\gamma_\mu A^\mu + \frac{\kappa_\tau}{2M}\sigma_{\mu\nu}\partial^\nu A^\mu\right)N \\
\mathcal{L}_{\rho\pi\pi} &= -g_{\rho\pi\pi}\vec{\rho}_\mu\cdot(\vec{\pi}\times\overleftrightarrow{\partial}^\mu\vec{\pi})/2 \\
\mathcal{L}_{\gamma\pi\pi} &= e\varepsilon_{3ij}A_\mu(\pi_i\overleftrightarrow{\partial}^\mu\pi_j) \\
\mathcal{L}_{\rho\gamma\pi} &= e\frac{g_{\rho\gamma\pi}}{m_\pi}\vec{\pi}\cdot(\varepsilon_{\mu\nu\rho\sigma}(\partial^\rho A^\mu)(\partial^\sigma\vec{\rho}^\nu)) \\
\mathcal{L}_{\omega\gamma\pi} &= e\frac{g_{\omega\gamma\pi}}{m_\pi}\pi^0(\varepsilon_{\mu\nu\rho\sigma}(\partial^\rho A^\mu)(\partial^\sigma\omega^\nu)) \\
\mathcal{L}_{\rho\gamma\eta} &= e\frac{g_{\rho\gamma\eta}}{m_\pi}\eta\left(\varepsilon_{\mu\nu\rho\sigma}(\partial^\rho A^\mu)(\partial^\sigma\rho^{0\nu})\right) \\
\mathcal{L}_{\rho\gamma\sigma} &= e\frac{g_{\rho\gamma\sigma}}{m_\rho}(\partial^\mu\rho^\nu\partial_\mu A_\nu - \partial^\mu\rho^\nu\partial_\nu A_\mu) \\
\mathcal{L}_{\rho\rho\gamma} &= 2e(A^\mu(\partial_\mu\rho_\nu)\tau_0\rho^\nu - (\partial^\nu A^\mu)\rho_\nu\tau_0\rho_\mu \\
&\quad + (\partial^\nu A^\mu)\rho_\mu\tau_0\rho_\nu)
\end{aligned} \tag{1}$$

For all channels discussed here we include a complete set of s-, u- and t-channel Born diagrams. In the photon and  $\rho$ -nucleon vertices form-factors for the magnetic contributions are included. The form-factors for the convection current contributions are implemented through the use of counter terms.

Currently we do not include direct matrix elements between the  $\rho - N$  and kaon sector. Because of the relatively weak coupling, as compared to the pion sector, this will not affect our main results. Also the final state interaction for the  $\rho - N$  state is not included. In the photo-induced  $\eta$  production channel we have taken into account an additional  $\rho$ -meson t-channel contribution in order to keep consistency with other channels. The value of the coupling constant  $g_{\rho\eta\gamma}$  was taken from decay data.

## A. The $\gamma + N \rightarrow \rho + N$ reaction channel

### 1. Born-level contributions and contact terms

Since we do not assign form factors to the convection current part of the  $\rho$  and photon vertices at the Born level, the pure convection current contribution is gauge invariant. However, the terms where one of the vertices is magnetic, are suppressed by form-factors and are subject to a gauge restoration procedure. The contact term required to restore gauge invariance reads

$$\begin{aligned}
C_{\rho^0}^{\mu\nu} &= -e\frac{g_{NN\rho}\kappa_\rho}{2m}\sigma^{\nu\lambda}k_\lambda\left[(2p+q)^\mu F_m^M(s)\tilde{f}_m^M(u)\right. \\
&\quad \left. + (2p'-q)^\mu F_m^M(u)\tilde{f}_m^M(s)\right] \\
&\quad - \frac{g_{NN\rho}\kappa_p}{2m}\sigma^{\mu\lambda}q_\lambda\left[(2p'-k)^\nu F_m^M(s)\tilde{f}_m^M(u)\right. \\
&\quad \left. + (2p+k)^\nu F_m^M(u)\tilde{f}_m^M(s)\right], \tag{2}
\end{aligned}$$

$$\begin{aligned}
C_{\rho^+}^{\mu\nu} &= -e\frac{g_{NN\rho}\kappa_\rho}{2m}\sigma^{\nu\lambda}k_\lambda\left[(2k-q)^\mu F_m^M(s)\tilde{f}_{m_\rho}^M(t)\right. \\
&\quad \left. + (2p'-q)^\mu F_{m_\rho}^M(t)\tilde{f}_m^M(s)\right] - e\frac{g_{NN\rho}\kappa_p}{2m}\sigma^{\mu\nu}F_{m_\rho}^M(t) \\
&\quad - g_{NN\rho}\frac{\kappa_\rho F_{m_\rho}^M(t) - \kappa_p F_m^M(s) + \kappa_n F_m^M(u)}{2m}\sigma^{\mu\lambda}q_\lambda\frac{k^\nu}{m_\rho^2}. \tag{3}
\end{aligned}$$

Where  $\tilde{f}_m^M(s)$  is defined as  $\tilde{f}_m^M(s) = (1 - F_m^M(s))/(s - m^2)$  and the form-factors are given in Eq. (6). Note, that the last term of Eq. (3) does not contribute to physical observables and serves only gauge invariance restoration purposes. We should note that this contact term is not unique and the exact functional form strongly depends on the ordering of terms in the minimal substitution procedure [16, 17, 18]. The present functional form is chosen to resemble the structure of the contact term used in kaon production, see Eq. (11a) and Eq. (11b) of ref. [16]. To present this contact term in a more readable way, we have given it for the  $\rho^0$  and  $\rho^+$  production channels separately.

In order to reproduce experimental data at high energies one also has to suppress the convection current contributions with form-factors. For this we have chosen to implement a prescription similar to the one proposed by Davidson and Workman [19]. Written as a gauge-invariant contact term [16] it reads

$$\begin{aligned}
C_{DW}^{\mu\nu} &= -eg_{NN\rho}\left[4\gamma^\nu(p\cdot qp'^\mu - p'\cdot qp^\mu)\right. \\
&\quad \left. - (2p\cdot q(\gamma^\mu\cancel{q}\gamma^\nu) + 2p'\cdot q(\gamma^\mu\cancel{q}\gamma^\nu))\right] \\
&\quad \times \left((1 - e_\rho)\tilde{f}_m(s)\tilde{f}_m(u) - e_\rho\tilde{f}_m(s)\tilde{f}_{m_\rho}(t)\right), \tag{4}
\end{aligned}$$

where  $\tilde{f}_m(s) = (1 - F_m(s))/(s - m^2)$ . This also gave good results for kaon production.

In order to achieve a better suppression of the u-channel contributions in the region of high momentum

transfer we have chosen to implement “modified” form-factors, as was done in the case of kaon production. The s-channel form-factor is redefined primarily for consistency considerations. This has hardly any effect on the results of the calculation, which are very similar to those obtained with the unmodified s-channel form-factor.

$$\begin{aligned} F_m(s) &= \frac{s\Lambda^2}{(\Lambda^2 + (s - m^2)^2)m^2}, \\ F_m(u) &= \frac{u\Lambda^2}{(\Lambda^2 + (u - m^2)^2)m^2}, \\ F_m(t) &= \frac{\Lambda^2}{\Lambda^2 + (t - m^2)^2}. \end{aligned} \quad (5)$$

The magnetic moments are suppressed by the quadrupole form-factors defined as

$$\begin{aligned} F_m^M(s) &= \left( \frac{s\Lambda^2}{(\Lambda^2 + (s - m^2)^2)m^2} \right)^2, \\ F_m^M(u) &= \left( \frac{u\Lambda^2}{(\Lambda^2 + (u - m^2)^2)m^2} \right)^2, \\ F_m^M(t) &= \left( \frac{\Lambda^2}{\Lambda^2 + (t - m^2)^2} \right)^2. \end{aligned} \quad (6)$$

All form-factors entering equations (2-4) use the same, relatively hard, cut-off of  $\Lambda = 0.8 \text{ GeV}^2$ .

## 2. Additional t-channel contributions

In addition to the Born-level contributions described above we include a number of t-channel contributions. At the higher energies, t-channel Regge exchanges are becoming more important and thus we include the Regge propagator for the dominant  $\sigma$ -meson t-channel exchange. In addition  $\pi$  and  $\eta$  t-channel exchanges are included, however these are of less importance.

Matrix elements for  $\eta$  and pion-exchange diagrams, following from the interaction Lagrangian (Eq. (1)), are given by

$$\begin{aligned} M_\phi^{\mu\nu} &= ig_{NN\phi} \frac{eg_{\rho\phi\gamma}}{m_\pi} \varepsilon^{\mu\nu\alpha\beta} k_\alpha q_\beta \frac{1}{t - M_\phi^2} \\ &\quad \times \bar{u}(p') \gamma^5 \frac{\not{p}' - \not{p}}{2M_N} u(p) F_{m_\phi}(t), \end{aligned} \quad (7)$$

where  $\phi$  is either  $\eta$  or  $\pi$  and  $F_{m_\phi}(t)$  is a dipole-type form-factor as is presented in Eq. (5). For both  $\eta$  and  $\pi$  contributions a hard cut-off of  $0.8 \text{ GeV}^2$  was used (the exact value does not matter much, and was chosen for consistency reasons).

The matrix element corresponding to  $\sigma$ -meson exchange, following from the interaction Lagrangian reads

$$\begin{aligned} M_\sigma^{\mu\nu} &= g_{NN\sigma} \frac{g_{\rho\sigma\gamma}}{M_\rho} (k \cdot q g^{\mu\nu} - q^\nu k^\mu) P_\sigma(s, t) \\ &\quad \times \bar{u}(p') u(p) F_{m_\sigma}(t), \end{aligned} \quad (8)$$

where  $F_{m_\sigma}(t)$  is the same dipole t-channel form-factor of Eq. (5) with cut-off set to  $1 \text{ GeV}^2$ . The Regge propagator  $P_\sigma(s, t)$  is defined as [20, 21]

$$P_\sigma(s, t) = \left( \frac{s}{s_0} \right)^{\alpha_\sigma(t)} \frac{\pi \alpha'_\sigma}{\Gamma(1 + \alpha_\sigma(t))} \frac{e^{-i\pi\alpha_\sigma(t)}}{\sin(\pi\alpha_\sigma(t))}, \quad (9)$$

where  $\alpha_\sigma(t)$  is  $\sigma$ -meson Regge trajectory defined as  $\alpha_\sigma(t) = \alpha_\sigma^0 + \alpha'_\sigma t$  with a slope of  $\alpha'_\sigma = 0.7 \text{ GeV}^{-2}$  and intercept of  $\alpha_\sigma^0 = -\alpha'_\sigma m_\sigma^2 = -0.4$ . The coupling constants  $g_{NN\sigma}$  and  $g_{\rho\sigma\gamma}$  are given in Table I. The reference scale  $s_0$  is conventionally chosen to be  $1 \text{ GeV}^2$ .

## B. The $\pi + N \rightarrow \rho + N$ reaction channel

Similar to the  $\gamma + N \rightarrow \rho + N$  reaction channel, the Born-level contributions include form-factors for the magnetic moment while the convection current contributions are suppressed by counter terms.

The  $\rho$ -meson, unlike the photon, couples with a different strength to the nucleon (in s- and u-channel contributions) and pion (t-channel contribution). As a result gauge invariance is obeyed only when  $g_{NN\rho} = 2g_{\rho\pi\pi}$ . To ensure gauge invariance for arbitrary values of the coupling constants we have introduced following contact term (putting  $\chi = 0$ )

$$\begin{aligned} C^\nu &= \frac{1}{4m} \left( -g_{NN\pi} (2g_{NN\rho} - g_{\rho\pi\pi}) (\not{q} + \not{k}) \gamma^5 \right. \\ &\quad \left. + 2g_{NN\rho} g_{NN\pi} \not{k} \gamma^5 \right) \frac{k^\nu}{m_\rho^2} (\vec{\tau}_N \cdot \vec{\tau}_\pi). \end{aligned} \quad (10)$$

This particular choice for the contact term gives a vanishing contribution to physical observables. However the choice of the contact term is ambiguous, where the ambiguity can be expressed as

$$C^\nu = g \frac{\gamma^\nu - \not{k} k^\nu / m_\rho^2}{2m} \gamma^5 (a + b \vec{\tau}_N \cdot \vec{\tau}_\pi), \quad (11)$$

where  $g$ ,  $a$  and  $b$  are arbitrary parameters. To fix the parameters we use the fact that a similar contact term appeared in kaon photoproduction. Exploiting the analogy between  $\rho$ -meson production and photo-induced kaon production we have fixed the parameters for our full calculation as  $g = g_{NN\pi} g_{\rho\pi\pi}$ ,  $a = 0$  and  $b = 1/2$ . Later in Section III we discuss the effects of this contact term on the results in more detail.

To implement form-factors for the convection current contributions we rewrite them first in terms of gauge-invariant amplitudes (these do not exactly correspond to  $M_i$  of photo-induced kaon production, although they are quite similar). For the part of the convection current contribution which corresponds to the  $A_2$  amplitude of kaon production, we implement the DW-style suppression scheme [19]. However, due to the more complicated

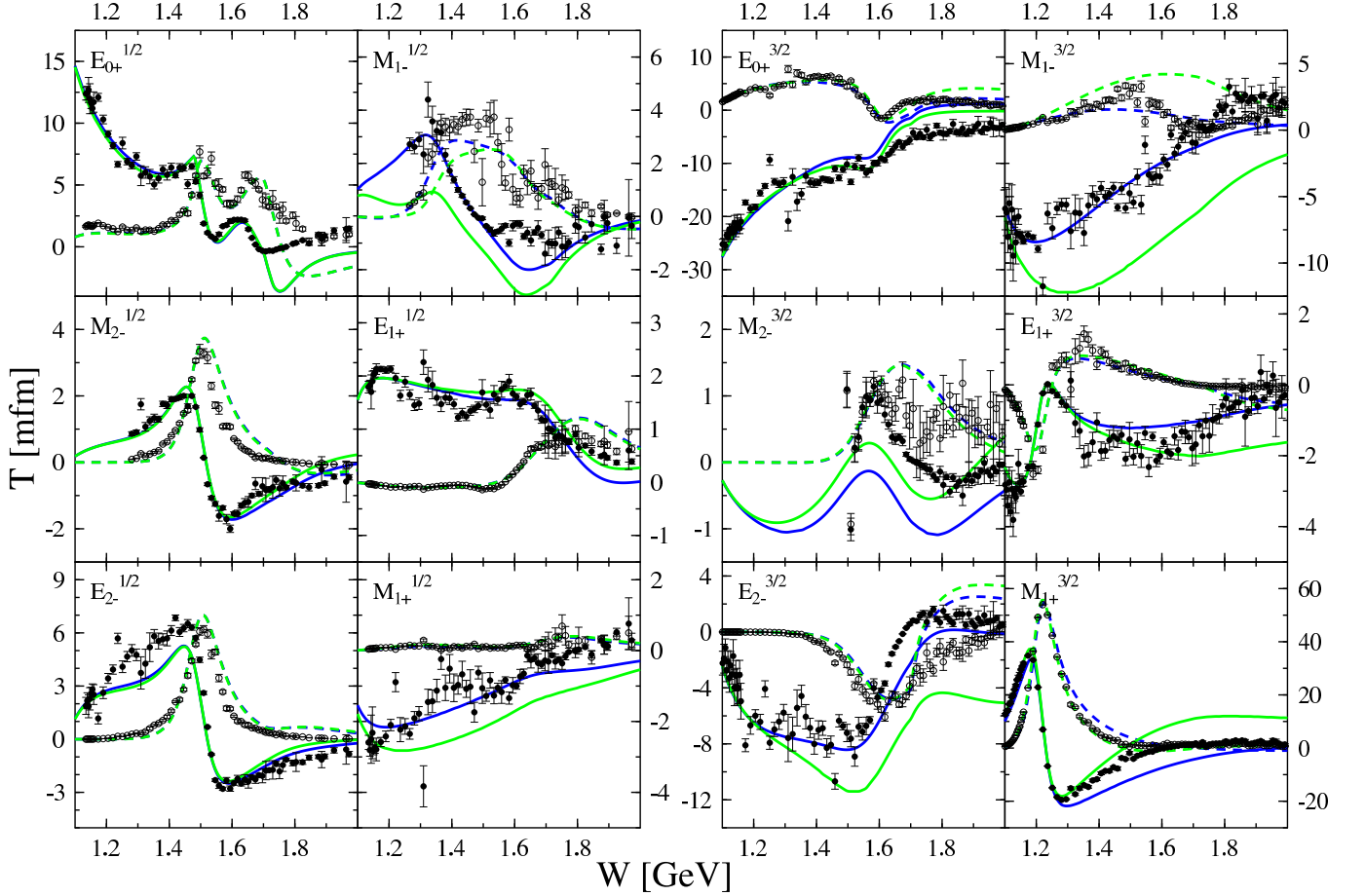


FIG. 1: [Color online] Partial wave decomposition of the  $\gamma + N \rightarrow \pi + N$  reaction channel. Solid and dashed lines correspond to the real and imaginary parts of the matrix element respectively. Darker (blue) lines shows the results of the new calculation, while lighter (green) lines correspond to the calculation where the tree-level  $\gamma + N \rightarrow \pi + N$  reaction channel agrees with that of [16]. The data are taken from the on-line database of the VPI group [22].

structure (in the general case of  $g_{NN\rho} \neq 2g_{\rho\pi\pi}$ ) we assign them a common overall form-factor  $F_{sut}^{DW}$  [19]. The corresponding contact term reads

$$\begin{aligned}
 C_{DW}^\nu = & \left[ -\frac{g_{NN\rho}g_{NN\pi}}{4m} \not{q}\gamma^5 \left( \frac{(2p+k)^\nu}{s-m^2} (1 - \vec{\tau}_N \cdot \vec{\tau}_\pi) \right. \right. \\
 & \left. \left. + \frac{(2p'-k)^\nu}{u-m^2} (1 + \vec{\tau}_N \cdot \vec{\tau}_\pi) - 4\frac{k^\nu}{m_\rho^2} (\vec{\tau}_N \cdot \vec{\tau}_\pi) \right) \right. \\
 & \left. - \frac{g_{NN\pi}g_{\rho\pi\pi}}{4m} (\not{q} + \not{k})\gamma^5 \frac{2q^\nu - 2q \cdot k k^\nu / m_\rho^2}{t-m^2} (\vec{\tau}_N \cdot \vec{\tau}_\pi) \right] \\
 & \times \tilde{f}_m(s)\tilde{f}_m(u)\tilde{f}_{m_\pi}(t)(s-m^2)(u-m^2)(t-m_\pi^2). \quad (12)
 \end{aligned}$$

The remaining contributions of the convection current are suppressed by individual form-factors through the in-

clusion of the following contact term

$$\begin{aligned}
 C^\nu = & -\frac{g_{NN\rho}g_{NN\pi}}{4m} \left[ \not{q}\gamma^5 \frac{k^\nu\gamma^\nu - \gamma^\nu k^\nu}{2} \tilde{f}_m(s)(1 - \vec{\tau}_N \cdot \vec{\tau}_\pi) \right. \\
 & \left. + \frac{k^\nu\gamma^\nu - \gamma^\nu k^\nu}{2} \not{q}\gamma^5 \tilde{f}_m(u)(1 + \vec{\tau}_N \cdot \vec{\tau}_\pi) \right]. \quad (13)
 \end{aligned}$$

In addition, for the reasons discussed in the results section, we include an extra contact term of the following form

$$C^\nu = -g_{NN\pi}g_{\rho\pi\pi}\gamma^5 \frac{2q^\nu - 2q \cdot k k^\nu / m_\rho^2}{m_\rho^2} (a + b\vec{\tau}_N \cdot \vec{\tau}_\pi) F_m(t), \quad (14)$$

where  $a = 1/3$  and  $b = 5/6$ .

In the  $\pi + N \rightarrow \rho + N$  reaction channel we do not use modified u-channel form-factors. The reason is that the effect of their inclusion is quite small and we opted for the simpler choice of dipole form-factors.

### C. The $\gamma + N \rightarrow \pi + N$ reaction channel

To improve the cross-sections at high energy we have introduced additional quadrupole form-factors for the magnetic moment contributions and used a “modified” u-channel form-factor. In addition, the cut-off value for the form-factors entering “core” contributions (s-, u-, t-channel contributions, gauge-invariance restoration and DW-contact terms) was reduced to  $0.8 \text{ GeV}^2$  and the  $NN\omega$  coupling constant was reduced by a substantial factor, as compared with the previous calculation.

### III. RESULTS

As the dominant source of indirect contributions to the  $\gamma + N \rightarrow \rho + N$  channel we identify the  $\gamma + N \rightarrow \pi + N \rightarrow \rho + N$  re-scattering process. Before addressing photo-induced  $\rho$ -meson production results, we discuss the results for pion photoproduction and pion-induced  $\rho$ -meson production, as these processes are crucial for the correct description of coupled-channels effects in the  $\rho$  photoproduction channel.

In Fig. 1 we compare partial wave data [22] with calculations for pion photoproduction at lower energies ( $W \leq 2 \text{ GeV}$ ). Shown are the results of the full calculation (darker blue line) and the results of the calculation where the tree-level description of the  $\gamma + N \rightarrow \pi + N$  channel agrees with that of ref. [16] (lighter green line, the “old” calculation). Note that due to the difference in treatment of coupled channels (primarily  $\pi + N \rightarrow \rho + N$  reaction channel) the results of the “old” calculation differs slightly from what was presented in ref. [16]. The present calculation, where some parameters were refitted, gives a considerable improvement in most partial wave amplitudes. The most important ingredients of the refitting are the suppression of  $\omega$ -meson t-channel contribution and the introduction of modified u-channel form-factors – they have impact on all partial waves. The softening of form-factors and introduction of quadrupole form-factors for magnetic moment contributions are most visible in the highest-energy tail of  $E_{0+}^{3/2}$ ,  $M_{1-}^{3/2}$ ,  $E_{2-}^{3/2}$  and  $M_{1+}^{3/2}$  amplitudes.

The results of the refitting are illustrated in some more detail in Fig. 2. The solid line shows the results of the final calculation. The calculation depicted with a dashed line uses non-modified (dipole) u-channel form-factors, which results in the unrealistically strong backward peaking of the differential cross-section. The dash-dotted line in Fig. 2 shows the results of the calculation in which the  $g_{NN\omega}$  coupling constant is increased to 8. This shows a too strong forward peaking. Despite the form-factor included in the  $\omega$ -meson t-channel contribution, the peak in the forward direction increases with the energy. We have investigated the possibility of including the Regge trajectory for the  $\omega$ -meson t-channel contribution, and although it suppresses the growth of the forward peak

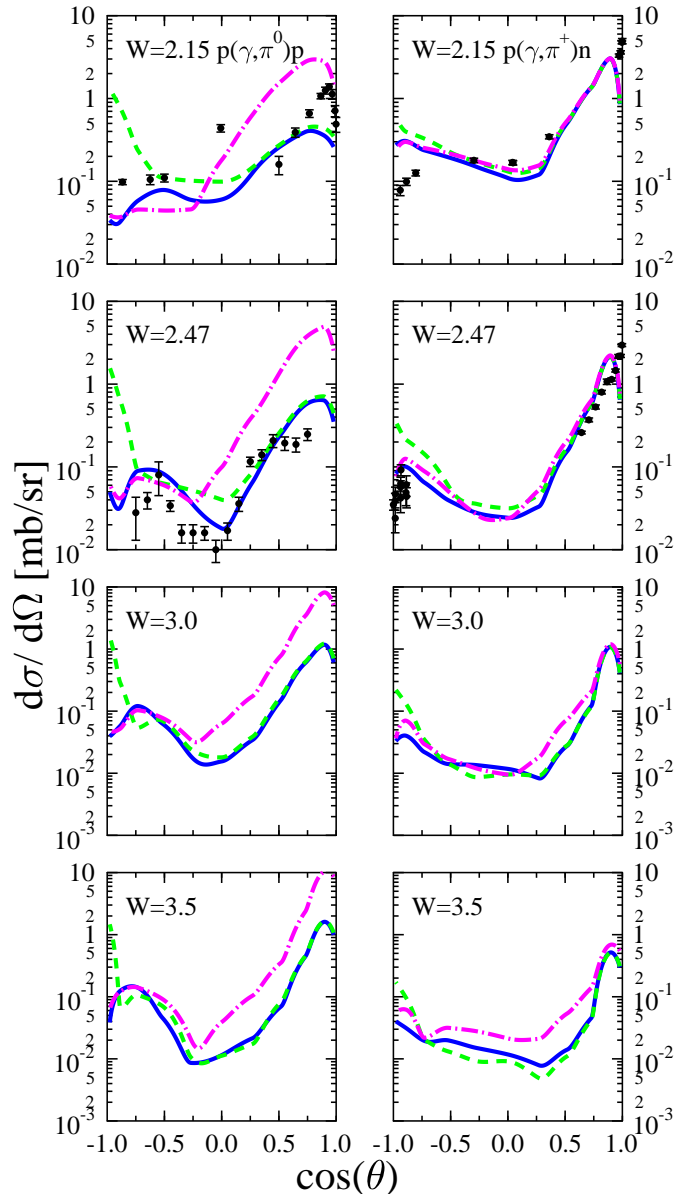


FIG. 2: [Color online] Differential cross-sections of the  $\gamma + N \rightarrow \pi + N$  reaction channel. See the text for the explanation of different curves. The data are taken from the on-line database of the VPI group [22].

with increasing energy, the numerical difference in the considered energy region is small and we decided to adopt the simpler option of using dipole-type form-factors. The impact of other changes, such as softening of form-factors and the use of quadrupole form-factors for magnetic moment contributions, is less visible in the cross-section plots, but result in visible changes in the partial waves decomposition.

In our approach the pion-induced  $\rho$  production channel is essentially parameters-free, where only the strength of additional gauge-invariant contact terms is adjusted. Un-

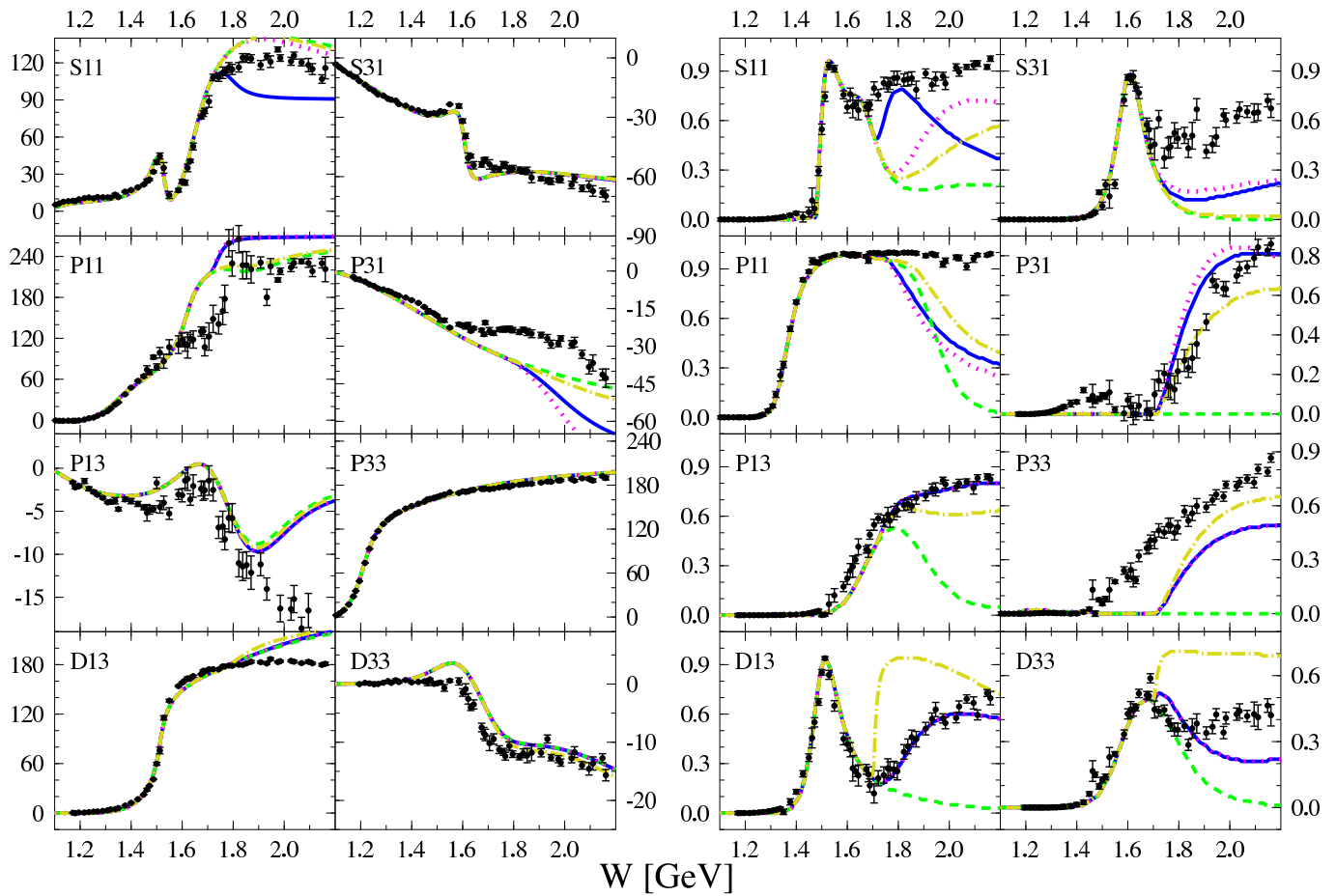


FIG. 3: [Color online] Partial wave decomposition for the  $\pi + N \rightarrow \pi + N$  reaction channel. The left plane shows per-partial wave phase shifts, and inelasticities are shown in the right plane. The solid (blue) line corresponds to the full calculation. The dashed (green) line shows the calculation where all reaction channels including  $\rho - N$  final state were excluded. The dotted (magenta) line denotes the calculation where an additional contact term of Eq. (11) is excluded from the  $\pi + N \rightarrow \rho + N$  reaction channel (note, that in spin-3/2 partial waves it agrees with the full calculation). The dash-dotted (yellow) line corresponds to the calculation where the contact term of Eq. (14) is excluded in the  $\pi + N \rightarrow \rho + N$  reaction channel. The data are taken from the on-line database of the VPI group[22].

fortunately there exists no direct experimental data for this channel and we rely on the inelasticities in pion scattering in order to constrain the parameters. As is shown in Fig. 3 (difference between solid and dashed lines) the inclusion of the  $\rho - N$  final state results in the generation of substantial inelasticities in pion scattering. The dash-dotted line in Fig. 3 shows the results of the calculation where the contact term of Eq. (14) is omitted in the pion-induced  $\rho$ -meson production channel. The effect of this contact term is to suppress the contribution of the t-channel, especially in the higher partial waves. An unrealistically steep rise of inelasticities in the higher partial waves shows that the inclusion of the contact term of Eq. (14) is vital for an accurate description of the experimental data.

For the pion-induced  $\rho$ -meson production channel there exist one more degree of ambiguity in constructing the gauge-invariance restoring terms as compared to photo-induced pion or kaon production. This ambiguity

we express as the contact term of Eq. (11). Excluding this contact term from the  $\pi + N \rightarrow \rho + N$  channel we obtain the result shown as the dotted line in Fig. 3. The impact of this contact term can also be observed in the kaon and  $\eta$  production channels, as is shown in Fig. 4, despite the fact that these are not coupled directly. While inclusion of this contact term seems to improve the description of  $K\Lambda$  and  $\eta$  production, it's effects on pion scattering and photoproduction channels are more controversial. The largest impact is seen in the  $S_{11}$  partial wave, where the description of the inelasticities improves at lower energies ( $W \simeq 1.8$  GeV), but becomes worse at higher energies ( $W > 2$  GeV). The impact on the  $S_{31}$  partial wave is quite small with the current choice of parameters, but could be of comparable strength. In other partial waves the effects are either small ( $P_{11}$  and  $P_{31}$  partial waves) or precisely zero (spin 3/2 and higher partial waves). In the pion photo-production sector the effect of this contact term is visible in  $E_{0+}^{1/2}$  and  $E_{0+}^{3/2}$

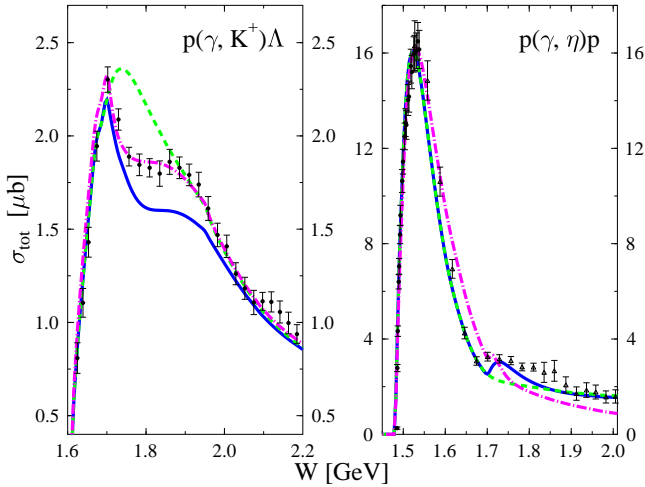


FIG. 4: [Color online] The effect of the contact term of Eq. (11) on kaon and  $\eta$  photoproduction. Solid (blue) line shows full calculation. Dashed (green) line corresponds to the calculation where contact term of Eq. (11) is excluded in  $\pi + N \rightarrow \rho + N$  reaction channel. The dash-dotted (magenta) line shows the results of the calculation as presented in our previous paper [16]. The data are taken from Refs. [23, 24].

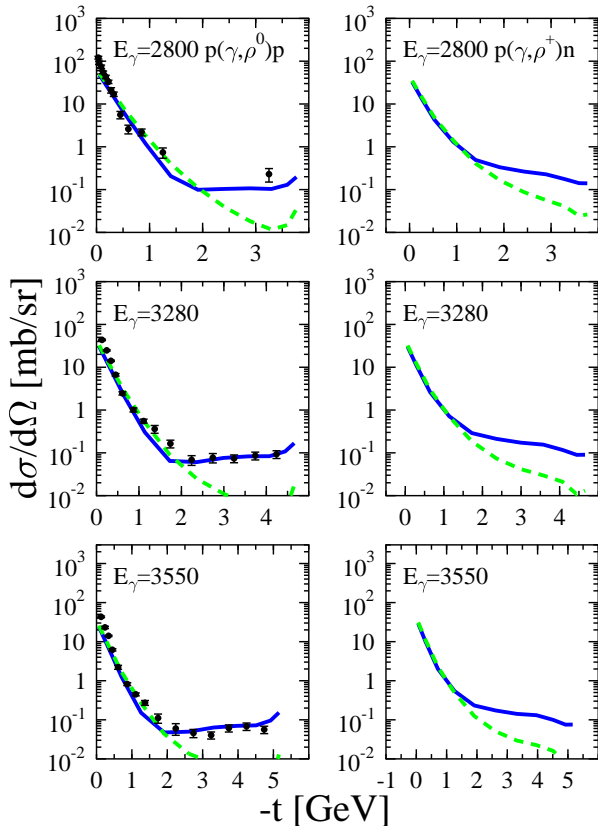


FIG. 5: [Color online] Differential cross sections for  $\rho$ -meson photoproduction. The solid line corresponds to the full calculation. The dashed line shows the tree-level calculation. Experimental data are taken from ref. [4]. The energies  $E_\gamma$  are given in MeV.

amplitudes at energies of  $W > 1.7$  GeV. In general the decision whether this contact term has to be included should be based on the results of a global fit, which will be presented in a forthcoming publication.

Inclusion of the contact term of Eq. (11), results in increased inelasticities in the pion sector, which is reflected in a dip in the photo-induced  $K\Lambda$  production cross-section at  $W = 1.7 - 2$  GeV, see Fig. 4. A more careful analysis on the level of partial waves reveals that the effect is seen primarily in S waves. Moreover, we have found that a similar suppression effect can be achieved by introducing an additional  $S_{11}$  resonance with appropriate parameters. While these two mechanisms (channel coupling effects and resonant contribution) give very similar results for the cross-sections and final state polarization, they are clearly distinguishable in the partial wave decomposition and could be separated given a full set of polarization observables. Some slight suppression of the final calculation compared to the one presented in ref. [16] (dash-dotted line) is due to somewhat increased inelasticities in pion sector. In order to minimize differences in the parameters we have decided to not refit kaon production channels, and are leaving this for the forthcoming publication.

In the  $\eta$  photoproduction channel, as shown in Fig. 4, the solid line represents the full calculation, and the dash-dotted line shows the results of the “old” calculation. The difference between them is primarily due to the inclusion of the  $\rho$ -meson t-channel contribution. Striking feature of the current calculation is the prominent peak at an energy of about  $W = 1.74$  GeV. To show the origin of this peak we present the results of a calculation where the contact term of Eq. (11) is excluded, shown as the dashed line in Fig. 4. This clearly demonstrates the peak is not a resonant contribution, but a channel coupling effect. It is interesting to note that this peak coincides in energy with the possible additional  $S_{11}$  resonance, as claimed in refs. [25, 26].

In Fig. 5 we present the results for the  $\gamma + N \rightarrow \rho + N$  channel. The dashed line corresponds to the tree-level calculation. Due to the use of modified u-channel form-factors and the use of DW-style suppression scheme we are able to get a similar description of the differential cross-section at the tree level, as obtained in ref. [14], while using much harder form-factors. The inclusion of Regge trajectory for the  $\sigma$ -meson t-channel contribution is essential for the correct description of the forward peak, and in the considered energy region allows to simulate the effects of the Pomeron contribution. Including the channel coupling effects results in the increase of the differential cross-section in the region of high momentum transfer, as is illustrated by the solid line. The coupled-channels result shows a good agreement with the data.

#### IV. CONCLUSION

We have extended the applicability of our coupled channels calculation to energies of the order of  $\sqrt{s} = 3.5$  GeV. A good agreement with experimental data is achieved for  $\gamma + N \rightarrow \rho + N$  reaction. We show that the channel coupling effects are extremely important in describing the experimental data on photo-induced  $\rho$ -meson production. In the kinematical regime of high momentum transfer it is the dominant contribution. As a primary source of indirect contributions we identify a re-scattering via an intermediate  $\pi - N$  state. Unfortunately there exist no direct data on pion-induced  $\rho$ -meson production in the energy regime up to  $\sqrt{s} = 3.5$  GeV. While it is possible to use the inelasticities induced in pion scat-

tering and pion production channel to constrain the implementation of pion-induced  $\rho$ -meson production channel, this still limits the accuracy of the predictions, as the magnitude of the re-scattering contributions is very sensitive to each of this channels.

The tendency of the coupled-channels calculation to enhance the cross-section at the large angles is very important for the correct comparison with the experimental data. As an example the comparison of the  $f_2$ -meson exchange with  $\sigma$ -meson exchange mechanisms presented as models “A” and “B” in ref. [14], shows that the main differences between them lie in the high momentum transfer region, where the coupled-channels contributions are playing dominant role.

- 
- [1] E. Anciant *et al.* [CLAS Collaboration], Phys. Rev. Lett. **85**, 4682 (2000) [arXiv:hep-ex/0006022].
- [2] K. Lukashin *et al.* [CLAS Collaboration], Phys. Rev. C **63**, 065205 (2001) [arXiv:hep-ex/0101030]. ;Phys. Rev. C **64**, 059901 (2001).
- [3] M. Battaglieri *et al.* [CLAS Collaboration], Phys. Rev. Lett. **87**, 172002 (2001) [arXiv:hep-ex/0107028].
- [4] M. Battaglieri *et al.* [CLAS Collaboration], Phys. Rev. Lett. **90**, 022002 (2003) [arXiv:hep-ex/0210023].
- [5] G. Penner and U. Mosel, Phys. Rev. C **66**, 055211 (2002) [arXiv:nucl-th/0207066].
- [6] G. Penner and U. Mosel, Phys. Rev. C **66**, 055212 (2002) [arXiv:nucl-th/0207069].
- [7] V. Shklyar, H. Lenske, U. Mosel and G. Penner, Phys. Rev. C **71**, 055206 (2005) [Erratum-ibid. C **72**, 019903 (2005)] [arXiv:nucl-th/0412029].
- [8] Q. Zhao, Z. p. Li and C. Bennhold, Phys. Rev. C **58**, 2393 (1998) [arXiv:nucl-th/9806100].
- [9] Q. Zhao, Phys. Rev. C **63**, 025203 (2001) [arXiv:nucl-th/0010038].
- [10] Q. Zhao, B. Saghai and J. S. Al-Khalili, Phys. Lett. B **509**, 231 (2001) [arXiv:nucl-th/0102025].
- [11] A. I. Titov and T. S. H. Lee, Phys. Rev. C **66**, 015204 (2002) [arXiv:nucl-th/0205052].
- [12] A. I. Titov and T. S. H. Lee, Phys. Rev. C **67**, 065205 (2003) [arXiv:nucl-th/0305002].
- [13] Y. s. Oh and T. S. H. Lee, Phys. Rev. C **66**, 045201 (2002) [arXiv:nucl-th/0204035].
- [14] Y. s. Oh and T. S. H. Lee, Phys. Rev. C **69**, 025201 (2004) [arXiv:nucl-th/0306033].
- [15] S. Capstick and W. Roberts, Prog. Part. Nucl. Phys. **45**, S241 (2000) [arXiv:nucl-th/0008028].
- [16] A. Usov and O. Scholten, Phys. Rev. C **72**, 025205 (2005) [arXiv:nucl-th/0503013].
- [17] S. Kondratyuk and O. Scholten, Nucl. Phys. A **677**, 396 (2000) [arXiv:nucl-th/0003009].
- [18] S. Kondratyuk and O. Scholten, Phys. Rev. C **62**, 025203 (2000) [arXiv:nucl-th/0001022].
- [19] R. M. Davidson and R. Workman, Phys. Rev. C **63**, 025210 (2001).
- [20] F. Cano and J. M. Laget, Phys. Lett. B **551**, 317 (2003) [Erratum-ibid. B **571**, 250 (2003)] [arXiv:hep-ph/0209362].
- [21] M. Guidal, J. M. Laget and M. Vanderhaeghen, Nucl. Phys. A **627**, 645 (1997).
- [22] R.A. Arndt, I.I. Strakovsky and R.L. Workman, Phys. Rev. C **53**, 430 (1996); **66**, 055213 (2002); updates available on the web: <http://gwdac.phys.gwu.edu>.
- [23] K. H. Glander *et al.*, Eur. Phys. J. A **19**, 251 (2004) [arXiv:nucl-ex/0308025].
- [24] V. Crede *et al.* [CB-ELSA Collaboration], Phys. Rev. Lett. **94**, 012004 (2005) [arXiv:hep-ex/0311045].
- [25] B. Saghai and Z. p. Li, Eur. Phys. J. A **11**, 217 (2001) [arXiv:nucl-th/0104084].
- [26] G. Y. Chen, S. Kamalov, S. N. Yang, D. Drechsel and L. Tiator, Nucl. Phys. A **723**, 447 (2003) [arXiv:nucl-th/0210013].